Conf-950336--25

EXPERIMENTAL EVALUATION OF A SIMULATION MODEL FOR WRAP-AROUND HEAT EXCHANGER, SOLAR STORAGE TANKS

Jeffrey A. Miller and Douglas C. Hittle
Solar Energy Applications Laboratory
Colorado State University
Fort Collins, Colorado

ABSTRACT

The thermal performance of a commercially available 80 gallon, solar storage tank with an integral wrap-around heat exchanger is characterized experimentally on an indoor test stand. The experimental results are used to evaluated the accuracy of a previously developed simulation model (Miller et al., 1993). Heat input on the collector side of the heat exchanger is held constant causing the heat transfer to reach a quasi-steady state. Temperatures in the heat exchanger and tank increase with time, however, the temperature differences across the heat exchanger remain nearly constant. Several combinations of heat input and collector loop flow are investigated. The development of the tank temperature profiles over time and the overall heat transfer performance predicted by the model are compared with experimental results. The influence of an electric auxiliary heater located in the top of the solar storage tank on the heat exchanger performance is investigated. Experimental normalization of the model is considered and modifications to the model and experiments are recommended.

NOMENCLATURE

A	surface area, m^2
C_p	specific heat, J/kg-K
D	diameter of the heat exchanger tubing, m
g	gravitational acceleration, m/s^2
Gr	Grashof number
h	heat transfer coefficient, W/K
k	thermal conductivity, W/m^2-K
L	height of the heater exchanger coil, m
M	mass of fluid, kg
$\dot{m}$	mass flow rate, kg/s
Nu	Nusselt number
Pr	Prandtl number
Q	heat transfer rate, W
Ra	Rayleigh number
Re	Reynold's number
T	temperature, K
UA	effective overall heat conductance, W/K
$\dot{V}$	volumetric flow rate, l/min
α	thermal diffusivity, m^2/s
β	volumetric thermal expansion coefficient, 1/K
γ	control function for makeup flow
ν	kinematic viscosity, m^2/s
η	overall surface efficiency
ρ	density, kg/m^3
Δ	difference

Subscripts

amb	ambient
aux	auxiliary heater
coil	heat exchanger coil segment
coll	collector loop
D	based on the diameter, D
env	storage tank environment
f	property of the fluid
hx	heat exchanger
i	tank segment index
in	inlet of the heat exchanger segment
L	makeup fluid (water from the main)
L	based on the length, L
lm	log mean
loss	loss to the tank environment
out	outlet of the heat exchanger segment
s	surface
tank	tank segment

MASTER

INTRODUCTION

The wrap-around heat exchanger solar storage tank consists of a typical 80 gallon (303 l) electric hot water heater tank with the

MASTER

CN= FG36-86SF16306
DOC=DOE/EE

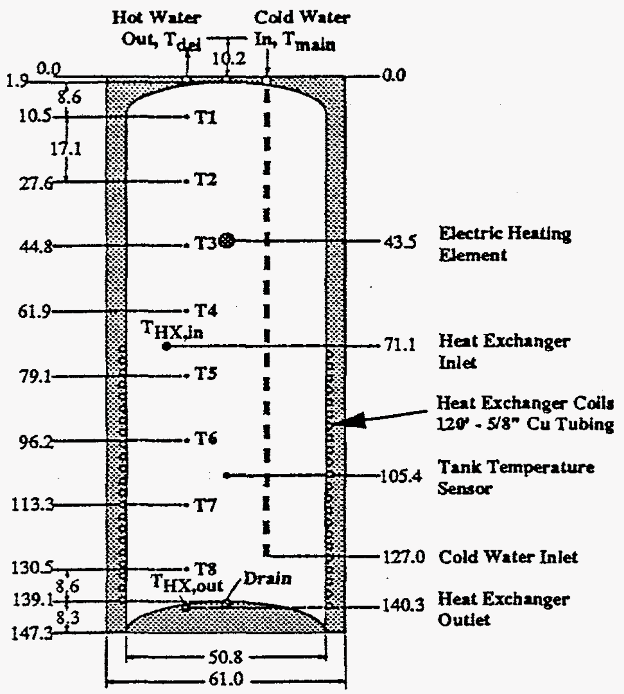

FIGURE 1. SCHEMATIC OF THE WRAP-AROUND HEAT EXCHANGER TANK. LOCATIONS OF THERMOCOUPLE TREE SENSORS ARE SHOWN. ALL DIMENSIONS IN CENTIMETERS

lower electric resistance heating element replaced by a 120 foot (36.6 m) long coil of 5/8 inch (1.59 cm) copper tubing wrapped around the outside of the lower half of the tank. The tank is shown schematically in Figure 1. The top third of the tank, heated by the remaining electric element, functions as an auxiliary tank. The bottom two-thirds is a solar pre-heat tank heated by hot antifreeze circulating from the solar collector through the external copper coil. This design provides a compact single tank system with an integral double-walled heat exchanger. No hot collector fluid flows through the tank to directly disturb the tank stratification. The wrap-around heat exchanger tank has become a popular option with solar domestic hot water system manufacturers and consumers.

TANK/HEAT EXCHANGER MODEL

The Type 4: Stratified Fluid Storage Tank model supplied with the solar simulation program, TRNSYS 13.1, has been modified to model this tank/heat exchanger combination (TRNSYS, 1990). The TRNSYS model divides the volume of the tank into N ($N \leq 15$) fully-mixed segments. An energy balance is performed on each segment which accounts for the flow of fluid into and out of the segment, the addition of auxiliary energy, and the loss of energy to the environment. In order to model the unique integration of the heat exchanger and solar storage tank, an additional term which accounts for heat transfer to each segment from the heat exchanger was included (Miller et al., 1993). This model is summarized below.

Energy Balance

For the wrap-around heat exchanger tank, an energy balance for the i th tank segment is expressed as,

$$M_i C_{p_f} \frac{dT_i}{dt} = \gamma_i \dot{m}_L C_{p_f}(T_L - T_i) + (1-\gamma_i)\dot{m}_L C_{p_f}(T_{i+1} - T_i) + (UA_i)_{loss}(T_{env} - T_i) + Q_{aux,i} + UA_{hx,i}\Delta T_{lm,i} \quad (1)$$

where T_i is the temperature of the i^{th} segment of the tank.

The first two terms on the left hand side of Eq. (1) account for the heat transferred to the i^{th} tank segment with the net fluid moving between tank segments as water is drawn from the tank. T_L *is the temperature of the mains water entering the bottom of the tank during a draw.* The control function, γ_i is equal to one for the tank segment receiving make-up water from the main supply and zero otherwise. No collector fluid enters the wrap-around heat exchanger tank.

The third term accounts for energy lost by heat transfer to the environment. The heat loss coefficient, U, is constant over the entire surface of the tank. A_i is the area around the perimeter of the i^{th} segment. For the first and last segments, this term includes additional heat loss through the top and bottom surfaces of the tank.

The fourth term, $Q_{aux,i}$, accounts for auxiliary heat added to segment i.

The last term accounts for heat transferred to the segment from the i^{th} segment of the heat exchanger coil. $UA_{hx,i}$ is the effective overall heat transfer conductance from the collector fluid to the domestic water in the tank and $\Delta T_{lm,i}$ is the log-mean temperature difference defined as

$$\Delta T_{lm,i} = \frac{(T_{coil,in,i} - T_i) - (T_{coil,out,i} - T_i)}{\ln\left(\frac{(T_{coil,in,i} - T_i)}{(T_{coil,out,i} - T_i)}\right)} \quad (2)$$

The inlet temperature to the first coil segment is an input to the tank model. The outlet temperature from the first coil segment is then calculated from an energy balance,

$$T_{coil,out,i} = T_{coil,in,i} - (T_i - T_{coil,in,i})\exp^{(-UA_{hx,i}/\dot{m}C_{p_f})} \quad (3)$$

and is the inlet temperature to the next coil segment.

Heat conduction between tank segments is not modeled.

Estimating $UA_{hx,i}$

Heat transfer between the hot fluid in the collector and the water in the tank is controlled by convective heat transfer in the tube, conduction through the tube and tank wall, and natural convection on the wall of the tank. The overall heat transfer coefficient can be estimated as (Incropera, 1990),

$$\frac{1}{UA_{hx,i}} = \frac{1}{(\eta hA)_{coil,i}} + R_{cond} + \frac{1}{(\eta hA)_{tank,i}} \quad (4)$$

The conductive heat transfer resistance of the tube and tank walls (R_{cond} in Eq (2)) is negligible when compared to the convective heat transfer resistances. $A_{coil,i}$ is the total area of the inside of the tube wrapped around the ith segment. $A_{tank,i}$ is the total surface area around the perimeter of the ith segment. The η's account for the overall surface efficiency of the respective surfaces. Surface efficiencies of one have been assumed.

The forced convection heat transfer coefficient is determined from the Gnielinski Nusselt number correlation for turbulent flow (Incropera, 1990),

$$Nu_D = \left(\frac{h_{coil}D}{k}\right) = \frac{(f/8)(Re_D - 1000)Pr}{1 + 12.7(f/8)^{1/2}\left(Pr^{2/3} - 1\right)} \tag{5}$$

where

$$f = (0.79 \ln Re_D - 1.64)^{-2}. \tag{6}$$

For constant fluid properties and a fixed tube geometry, h_{coil}, is approximately proportional to the fluid flow rate on the collector side raised to the 4/5 power.

Determining the natural convection heat transfer coefficient is less straightforward. General Nusselt number correlations for free convection on the inside surface of an enclosure with a stratified medium are not generally available. The correlation for free convection on a uniform temperature, vertical plate in an infinite medium is used to estimate the tank-side convection coefficient. For turbulent flow ($Ra_L > 10^9$) (Incropera, 1990),

$$Nu_L = \left(\frac{h_{tank}L}{k}\right) = 0.10 Ra_L^{1/3} \tag{7}$$

where the Rayleigh number, Ra_L, is given by,

$$Ra_L = Gr_L\, Pr = \frac{g\beta(T_s - T_i)L^3}{\nu\alpha}. \tag{8}$$

The natural convection boundary layer on the inside wall of the tank is assumed to extend over the height of the heat exchanger coil. When the height of the heat exchanger coil is used for the characteristic height, L, the Rayleigh number is typically much larger than 10^9, even for small temperature differences. Note, for turbulent flow, the free convection heat transfer coefficient becomes independent of the characteristic length L.

The presence of an enclosure and a stable temperature gradient will both act to retard the development of the natural convection boundary layer and reduce the natural convection heat transfer coefficient. This model is therefore expected to over predict the heat exchanger performance.

For fixed fluid properties, h_{tank} varies with the temperature difference, $(T_s - T_i)$, to the 1/3 power. The surface temperature of the tank wall, T_s, is estimated from a heat balance on the tank wall,

$$Q_{coil,i} = (\eta h A)_{coil,i}\left(\overline{T}_{coil,i} - T_s\right) = (\eta h A)_{tank,i}(T_s - T_i) \tag{9}$$

where, $\overline{T}_{coil,i}$ is the mean temperature of the fluid in the i^{th} coil segment. The temperature difference, $(T_s - T_i)$, is therefore a function of h_{tank}, and $h_{tank,i}$ and $(T_s - T_i)$ must be determined by iteration of Eqs. (7) and (9).

EXPERIMENTS

When the heat input to the collector side of the heat exchanger is held constant with no draw flow and no auxiliary heat addition, the overall energy balance (reference Eq. (1) above) on the solar portion of the tank becomes

$$MC_{p_r}\frac{dT}{dt} = UA_{hx}\Delta T_{lm} = Q_{input} = \text{constant} \tag{10}$$

For all cases of interest, tank losses are small compared to the heat gain across the heat exchanger. The tank temperature will increase linearly in time and for a fixed collector-side flow rate, the heat exchanger overall heat transfer coefficient, UA_{hx}, and log-mean temperature difference, ΔT_{lm}, will remain nearly constant over the length of the test. Increasing Q_{input} (from run to run) while holding the collector-side flow rate constant, increases the ΔT_{lm} and the tank-side free convection heat transfer coefficient, h_{tank}, independent of the coil-side, h_{coil}. Holding Q_{input} constant (from run to run) while increasing the collector-side flow rate increases the coil-side forced convection heat transfer coefficient, h_{coil}, although, not independent of the tank-side heat transfer. As h_{coil} increases the temperature difference driving the free convection flow will decrease (reference Eqs. (7)-(9)).

Apparatus and Instrumentation

The tank/heat exchanger was characterized on an existing indoor test stand (Davidson et al., 1993). On the collector side of the tank/heat exchanger, heat gain is simulated with a computer controlled circulation heater. Two cold water supply tanks allow the solar storage tank to be preconditioned at the start of a run and allow the temperature of the make-up water during domestic hot water draws to be controlled.

Eight special limit, T-type thermocouples (T1-T8) are located vertically in the tank as shown in Figure 1. They divide the tank into eight equal segments. The thermocouples are inserted through the 3/4" NPT hot water outlet fitting in individual 1/8 inch (3.175mm) brass sheaths. The open area of the outlet is reduced by approximately 25%. The thermocouple beads are electrically insulated from the sheath and from the water with thermocouple epoxy.

The tank environment temperature (T_{env}) is measured by a radiation shielded thermocouple at the mid-height of the tank.

Temperatures at the inlet and outlet of the circulation heater, the heat exchanger ($T_{hx,in}$ and $T_{hx,out}$) and the solar storage tank (T_{main} and T_{del}) are measured with prefabricated, 2252 ohm thermistors in 1/8 inch (3.175mm) stainless steel sheaths.

An end-to-end (computer to sensor) calibration was performed on all of the temperature sensors. The calibration uncertainty has been estimated at ±0.1 °C (Coleman et al., 1989).

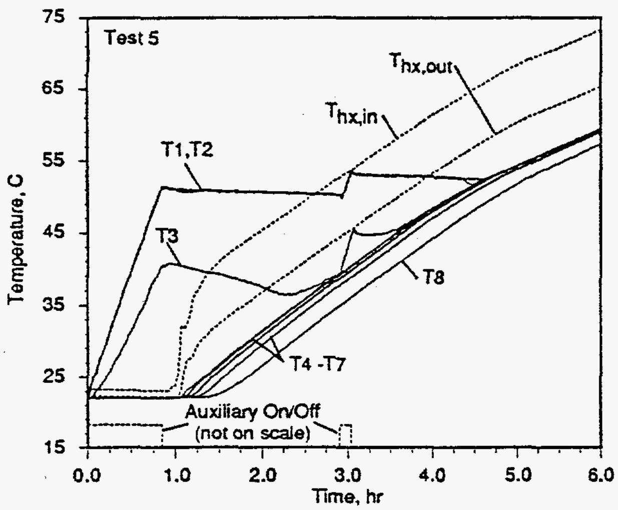

FIGURE 2. DEVELOPMENT OF TANK AND HEAT EXCHANGER TEMPERATURES FOR A TYPICAL CONSTANT HEAT INPUT TEST.

Water is the heat transfer fluid on the collector side of the heat exchanger, for the experiments reported here Turbine flow meters measure the collector loop volumetric flow rate and the draw volumetric flow rate. The flow meters are calibrated to ±0.06 lpm.

Watt transducers monitor the electrical power drawn by the circulation heater and the solar storage tank auxiliary heater (±1% of reading).

All of sensors were sampled at 10 sec intervals for the duration of the test.

Procedure

Figure 2 shows the history of the tank and heat exchanger temperatures for a typical constant heat input test (Test 5, Tables 1 and 2 below). The average heat input to the collector loop for this test was 2171 watts. The collector loop flow rate was 3.78 lpm (1.0 gpm).

At the beginning of the test, the auxiliary heater element is enabled to allow the top of the tank to reach normal operating condition. The temperatures at the top two thermocouple locations T1 and T2 (reference Figure 1), located above the heater element, rise together. Note, when the auxiliary heater initially shuts off, the bulk water temperature at T1 and T2 is not at the thermostat set point of 54 °C (130 °F). Later in the test, the auxiliary heater comes back on for a short time and the bulk water temperature does reach the thermostat set point. This response is typical of many electric hot water heaters. The thermostat measures the wall temperature of the tank just above the heater element, not the temperature of the water. On initial heat-up from a cold start, the wall temperature above the base of the element rises more quickly than the bulk fluid temperature and the thermostat appears to shut off the heater early. As the tank wall cools below the lower set point, the heater turns back on. The operation of the auxiliary heater does not seem to influence the heat transfer across the heat exchanger.

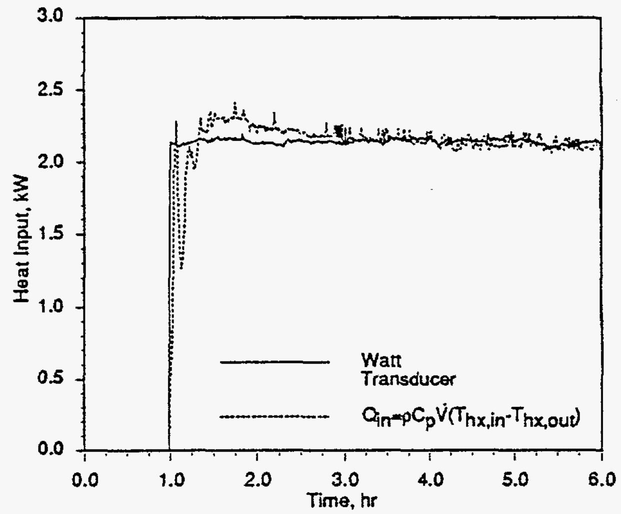

FIGURE 3. COMPARISON OF THE MEASURED ELECTRICAL POWER TO THE CIRCULATION HEATER WITH THE CALCULATED HEAT TRANSFER ACROSS THE HEAT EXCHANGER.

The temperature at thermocouple T3, just below and to the side of the heater element, is strongly influenced by the auxiliary heater. The temperature rises more slowly, however, and decays quickly when the heater shuts off due to conduction losses to the colder bottom of the tank.

One hour into the test, the circulation pump and heater are enabled. As heat is added, the water temperature in the lower half of the tank (T5 - T8) rises above the temperature of the water just above (T3 -T4). This temperature instability gives rise to free convection circulation which mixes the bottom and middle nodes of the tank. The portion of the tank heated by the auxiliary heater is not affected until the temperature of the lower portion of the tank rises above the auxiliary set point. At six hours, the circulation heater and pump are disabled. Throughout the test, the temperature at the bottom most thermocouple, T8, is several degrees lower than the remainder of the tank. This lag is due in part to increased losses through the bottom surface of the tank. Also, the fluid at the very bottom of the tank may not participate fully in the natural convection driven motion in the tank.

Figure 3 plots the measured electrical power drawn by the circulation heater and the heat transfer across the heat exchanger (calculated as shown in the figure). Although the electrical power input to the circulation heater is preset before the start of the experiment and remains nearly constant through out the test, the heat transfer across the heat exchanger is not entirely constant. Oscillations are visible in the calculated heat transfer at the start of the test. For historical reasons, the circulation heater is currently located two stories (approximately 9m (30 ft)) above the solar storage tank. At a flow rate of 3.78 lpm, the fluid takes on the order of three minutes to make a round trip. Initially, the temperature of the water in the 36.6 meters (120 ft) of heat exchanger tubing is at the tank starting temperature of 22 °C. The temperature of the water in the piping leading to and from the circulation heater may be two to three degrees warmer (in the summer) due to heat exchange with the ambient. Constant heat input to the collector loop at the circulation heater causes a fixed temperature rise across the heater. As cooler water from the heat exchanger reaches the inlet of the heater, the outlet temperature drops slightly and then rises again with rising inlet temperature. These oscillations may persist for as long as 30 minutes before a steady increase in outlet temperature is reached. The heat transfer across the heat exchanger also shows a slight decrease during the run as piping heat losses between the heater and the tank increase as the fluid heats up during the test.

MODEL COMPARISON

The model was configured to simulate the experiment shown in Figure 2. The height and diameter of the interior of tank are 1.37 m (54 in.) and 0.508 m (20 in.) respectively (reference Figure 1). The calculated volume of the solar tank is 278 l (73.44 gal.), approximately 92% of the nominal volume of 302 l (80 gal.). The height of the heat exchanger is 0.686 m (27 in). The appropriate heat loss coefficient of the tank was determined in a separate heat loss experiment to be 1.44 (W/m^2-K).

Eight equal sized tank segments were specified for the simulation to match the eight thermocouple measurements in the tank. Due to the high degree of mixing which occurs as heat is added, the simulation results for this tank are not highly sensitive to the number of segments modeled. The location of the auxiliary heater and thermostat was specified as the second (from the top) tank node (T2 in Figure 1). The reference value for the auxiliary heater power is 3200 W (4500 W de-rated for the 208 VAC service available on this test stand with a 95% efficiency). The thermostat set point and deadband were determined from experiment to be 54°C (130°F) and 3 °C (5°F).

The average volumetric flow rate in the collector loop (3.87 lpm) and tank environment temperature (23.9°C) measured in the experiment were specified as an input to the simulation.

In order to more closely model the experimental results, the variation in the heat transfer across the heat exchanger was calculated from the experimental results and input to the simulation.

Figure 4 shows the development of the tank and heat exchanger temperatures for a simulation of the experiment shown in Figure 2. The collector loop heat input and flow rate are specified from experimental values, so the temperature difference from the inlet to the outlet of the heat exchanger ($T_{hx,in}$ - $T_{hx,out}$) must be equal to the experimental value. The predicted temperature difference from the heat exchanger to the tank is, however, much smaller than observed ($T_{hx,out}$ lies much closer to the lower tank temperatures, T3-T7).

If an overall log-mean temperature difference across the heat exchanger is defined as

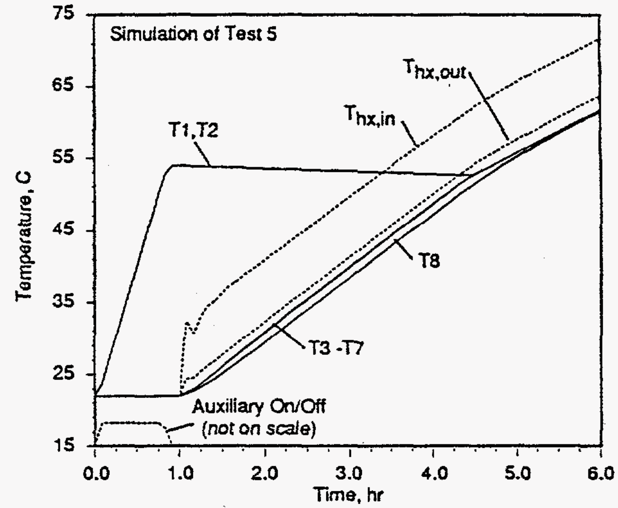

FIGURE 4 DEVELOPMENT OF TANK AND HEAT EXCHANGER TEMPERATURES FOR A SIMULATION OF THE CONSTANT HEAT INPUT TEST IN FIGURE 2.

$$\Delta T_{lm} = \frac{(T_{hx,in} - T_{tank,5}) - (T_{hx,out} - T_{tank,8})}{\ln\left(\dfrac{(T_{hx,in} - T_{tank,5})}{(T_{hx,out} - T_{tank,8})}\right)} \qquad (11)$$

the effective heat exchanger conductance is,

$$UA_{hx} = \frac{Q_{input}}{\Delta T_{lm}} \qquad (12)$$

These quantities are plotted in Figures 5 and 6, respectively, for Test 5. The trace of ΔT_{lm} shows some of the oscillations visible in the plot of Q_{input} (Figure 3). The effective heat exchanger conductance, UA_{hx}, does become nearly constant early on in the test. Figures 5 and 6 also show a plot of the log-mean temperature difference, ΔT_{lm}, and the overall heat exchanger conductance, UA_{hx}, calculated from the simulation results. The predicted value of UA_{hx}, is approximately twice as large as the measured value; consequently, ΔT_{lm} is 50% lower.

The slope of the temperature rise in the experimental tank is slightly smaller than the simulation. This indicates that the actual capacitance, MC_p, of the tank is slightly greater than calculated by the model.

Table 1 compares the average log-mean temperature difference, ΔT_{lm}, and effective overall heat exchanger conductance, UA_{hx}, determined from experiment to those predicted by simulation for several combinations of Q_{input} and $\dot{V}_{coll}$. In the first series, the heat input was varied from approximately 1000 W to 4000 W with the collector loop flow rate fixed at approximately 3.78 l (1 gpm). In the second series, the heat input was fixed at approximately 2000 W and the collector loop flow rate was varied. Note, results of Test 9 are merely an echo of Test 5.

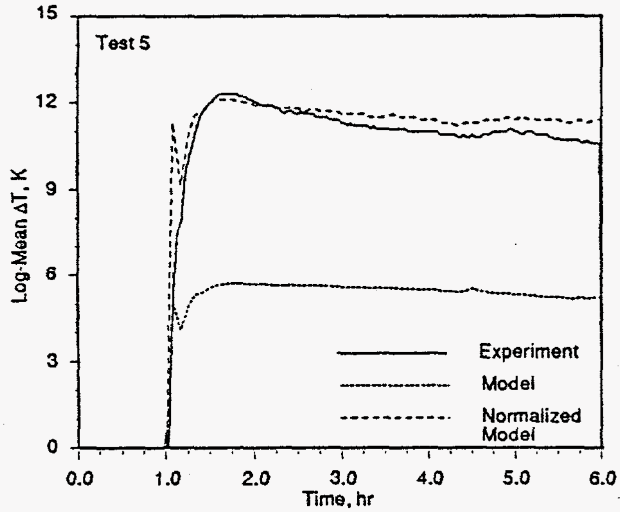

FIGURE 5. OVERALL LOG-MEAN TEMPERATURE DIFFERENCE, ΔT_{lm}, CALCULATED FROM MODEL RESULTS AND EXPERIMENTAL DATA.

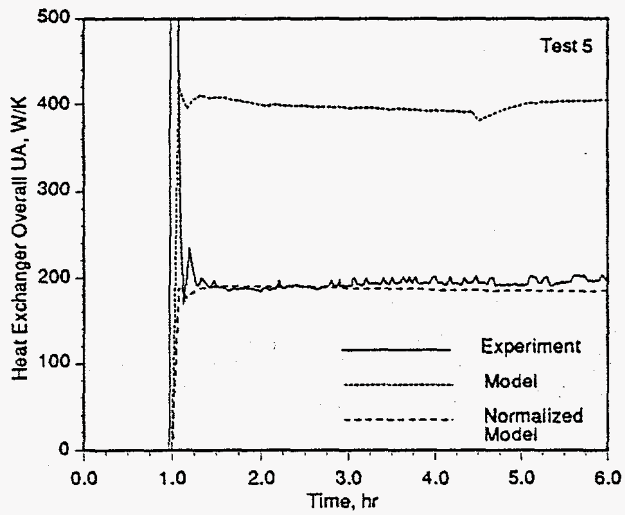

FIGURE 6. EFFECTIVE OVERALL HEAT EXCHANGER CONDUCTANCE, UA_{hx}, CALCULATED FROM MODEL RESULTS AND EXPERIMENTAL DATA.

The experimental values for UA_{hx} do not change greatly with either increasing ΔT_{lm} in the first series or with increasing collector flow rate in the second. The model consistently over predicts the effective heat exchanger conductance by a factor of 2.0 to 2.5. The effect of increasing ΔT_{lm} and increasing flow rate is more pronounced for the simulation results.

That the model described above predicts a larger heat exchanger UA_{hx} product than is observed is not surprising. On the coil side of the heat exchanger, the Nusselt number correlation employed (Eq. (5)) applies to uniform heat transfer around the circumference of the tube. Heat transfer occurs primarily on one

TABLE 1. COMPARISON OF MEASURED AND PREDICTED VALUES OF LOG-MEAN TEMPERATURE DIFFERENCE AND EFFECTIVE HEAT EXCHANGER CONDUCTANCE.

				Experiment		Simulation	
Test	Q_{input} W	Flow Rate lpm	Flow Rate gpm	ΔT_{lm} K	UA_{hx} W/K	ΔT_{lm} K	UA_{hx} W/K
1	893	3.77	1.0	5.2	173	2.6	337
2	1044	3.98	1.1	6.0	174	2.9	353
3	1762	3.66	1.0	9.7	183	4.7	376
4	1830	3.76	1.0	9.9	186	4.8	383
5	2171	3.78	1.0	11.2	193	5.5	397
6	2910	3.73	1.0	16.9	173	7.1	410
7	4171	3.7	1.0	23.4	178	9.3	451
8	2015	1.91	0.5	10.8	188	6.2	325
9	2171	3.78	1.0	11.2	193	5.5	397
10	2076	7.61	2.0	11.0	188	4.7	442
11	1991	11.78	3.1	10.9	182	4.4	444

side of the tube in this case. In addition, one would expect, based observation of the joint between the coil and the tank, that the overall surface efficiency, η_{coil} would indeed be less than one. The conduction heat transfer resistance through the bond and tank wall may indeed be significant. Perhaps most important, a Nusselt number correlation for free convection on a flat vertical surface in an infinite medium was used to estimate the heat transfer coefficient on the tank wall. The presence of the enclosure and the effect of the (slightly) stratified medium both inhibit the natural convection circulation in the tank and reduce the heat transfer coefficient.

Model Normalization

A procedure for normalizing this model to more closely simulate the observed performance characteristics of this combination of tank and heat exchanger has been considered. When Eq. (4) is rewritten as,

$$\frac{1}{\eta_0 UA_{hx,i}} = \frac{1}{\eta_1 (hA)_{coil,i}} + \frac{1}{\eta_2 (hA)_{tank,i}} \qquad (13)$$

the parameter η_0 adjusts the overall conductance calculated by the model, and the parameters η_1 and η_2 adjust the calculated conductance on the coil-side and tank-side of the heat exchanger respectively. With $\eta_0 = \eta_1 = \eta_2 = 1$, the model remains unchanged and the results of Table 1 and Figures 5 and 6 are obtained. For the results reported here, each parameter is modified independent of the remaining two (i.e the remaining two are fixed at 1). In each case, the standard estimate of error (root-mean-square error) between the measured and predicted overall log-mean temperature difference (Coleman et al., 1989),

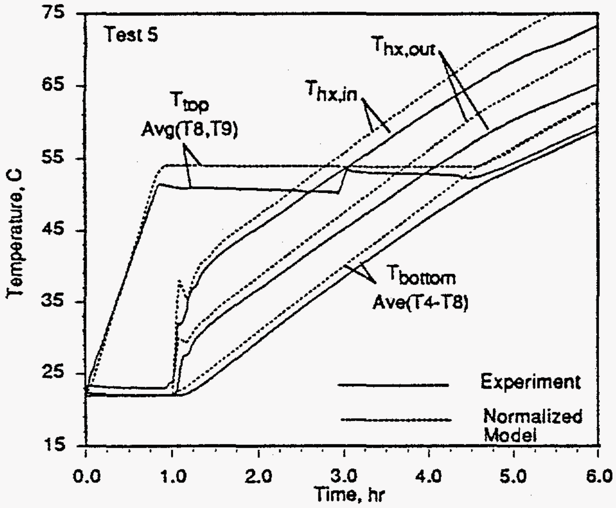

FIGURE 7. COMPARISON OF TANK AND HEAT EXCHANGER TEMPERATURES CALCULATED FROM "NORMALIZED" MODEL RESULTS WITH THE EXPERIMENTAL DATA.

$$SEE = \left(\frac{\sum_{1}^{N} (\Delta T_{lm,Experiment} - \Delta T_{lm,Model})^2}{N-1} \right)^{1/2} , \qquad (14)$$

is minimized to obtain the value of that parameter which gave the "best fit" between the simulation and the experiment. The standard estimate of error, SEE, is calculated over the interval starting 30 minutes after the circulation heater is enabled (to avoid the oscillations in at the beginning of the experimental data) and ending when the heater is disabled. Experimental and simulation values are compared every 5 minutes.

For Test 5 of Table 1 above, a value of η_0=0.38 (with $\eta_1=\eta_2$=1) minimizes the SEE (as defined in Eq. (14)) at 0.25 K. Figures 5 and 6 show the new predicted values of ΔT_{lm} and UA_{hx} overlaid on values from the experiment and from the nominal simulation. In Figure 7, the predicted tank and heat exchanger temperatures are compared to the (mean) experimental values. Note that the temperatures at thermocouples T8 and T9 are averaged to indicate a temperature characteristic of the tank above the auxiliary heater, and the temperature at thermocouples T4-T8 are averaged to indicate the temperature characteristic of the bottom of the tank.

The predicted temperatures do rise more quickly due to a difference between the actual capacitance, MC_p, of the tank and the capacitance of the volume of water modeled in the simulation. Overall agreement is now, however, very good. Note that the value of η_0 required to get a best "fit" is less than 0.49, the ratio of the experimental value of UA_{hx} to the simulation value in Table 1. This occurs because as the calculated value of UA_{hx} is reduced, ΔT_{lm} increases and, along with it, the natural convection term in Eq. (4). When either η_1 or η_2 is decreased, the heat

TABLE 2. RESULTS OF THE WRAP-AROUND HEAT EXCHANGER TANK MODEL "NORMALIZATION" FOR PARAMETERS η_0, η_1, AND η_2 IN EQ. (11).

Test	η_0	SEE K	η_1	SEE K	η_2	SEE K
1	0.42	0.34	0.07	0.31	0.39	0.34
2	0.41	0.19	0.06	0.15	0.38	0.20
3	0.38	0.57	0.07	0.54	0.34	0.58
4	0.38	0.57	0.07	0.52	0.34	0.57
5	0.38	0.25	0.07	0.22	0.35	0.26
6	0.30	0.29	0.06	0.31	0.27	0.29
7	0.29	0.45	0.06	0.47	0.25	0.45
8	0.46	0.64	0.14	0.59	0.40	0.64
9	0.38	0.25	0.07	0.22	0.35	0.26
10	0.35	0.18	0.04	0.15	0.33	0.19
11	0.32	0.08	0.02	0.45	0.31	0.09

transfer balance in Eq. (9) also shifts, further altering the ΔT which determines the natural convection coefficient.

Table 2 lists the values of η_0, η_1, and η_2 required to obtain agreement with the tests in Table 1. Remember, each parameter was adjusted independent of the others (i.e the remaining η's were equal to 1).

The heat transfer on the coil side of the heat exchanger (η_1 in Table 2) must be reduced by a factor of 20 to obtain good agreement the experiment. This reduction is too large to be explained by the surface efficiency of the coils, and suggests that the overall effective heat conductance of the heat exchanger is controlled by heat transfer on the tank side of the heat exchanger. The fact that a uniform value η_2 will not match all of the tests in the first series of tests (with fixed collector flow) suggests that the modeled temperature dependence of the tank side free convection coefficient is too strong. The results for η_0 show a similar trend to those for η_1.

RECOMMENDATIONS AND CONCLUSIONS

The current model of this unique combination of tank and heat exchanger clearly over-estimates the effective heat transfer conductance of this heat exchanger by a factor of 2 or more. A means of correcting the model and/or normalizing the model to the experimental data must be identified. These comparisons suggest that the model does in fact over estimate the free convection heat transfer on the tank side of the heat exchanger.

Several courses of action are possible. The UA in the model could be set at a fixed value determined from the experiments. The calculated values of UA_{hx} tabulated in Table 1 do not vary greatly with either collector flow rate or heat input. The modeled heat transfer performance would, however, no longer depend on the flow rate in the collector loop or the temperature difference across the heat exchanger. To maintain these dependencies, one or both of η_1 and η_2 could be adjusted to scale the individual heat transfer correlations. The results above suggest that η_2 which modifies the free convection heat transfer coefficient would be the mostly likely candidate. A modification of the ΔT dependence of this term should also be considered. Modification of a combination of the coil and tank side terms may also be necessary though more difficult. Finally, the magnitude of the conduction resistance should be re-evaluated.

In any case, a more complete data set should be acquired to insure that the resulting model is applicable over the widest possible range of operating conditions. Of particular interest is the performance of the heat exchanger with low collector flow rates.

In order to make a comparison of the simulation results with measured values, the experiment should be modified to reduce the heat loss in the piping between the heater and the tank and also to reduce the oscillation at the beginning of the test. In further testing, a test with constant temperature at the inlet of the heat exchanger should be considered. Such an experiment would vary the delta T across the heat exchanger continuously while the flow rate is held fixed.

Once model modifications are adopted, a simulated solar day test should be conducted to insure that the model works under the real world conditions.

REFERENCES

ASHRAE, 1989 Handbook of Fundamentals, American Society of Heating, Refrigerating and Air Conditioning Engineers, Inc., Atlanta, GA.

Coleman, H. W., and W.G.Steele Jr., *Experimentation and Uncertainty Analysis for Engineers*, John Wiley and Sons, Inc., New York, NY, 1989.

Davidson, J. H., W. T. Carlson, W. S. Duff, P. J. Schaefer, W. A. Beckman, and S. A. Klein, "Comparison of Experimental and Simulated Thermal Ratings of Drain-Back Solar Water Heaters," *Journal of Solar Energy Engineering*, Vol. 115, May 1993.

Duffie, J. A., and Beckman, W. A., 1991, *Solar Engineering of Thermal Process*, 2nd Ed., John Wiley & Sons, Inc., New York, NY.

Incropera, F. P. and DeWitt, D. P., 1990, *Fundamentals of Heat and Mass Transfer*, 3rd Ed.,John Wiley and Sons, New York, NY.

Miller, J. A., and D. C. Hittle, "Yearly Simulation of a PV Pumped, Wrap-Around Heat Exchanger, Solar Domestic Hot Water System," *Solar Engineering 1993, ASME/ASES/ISES Solar Energy Conference*, Washington, D.C., April 4-9, 1993.

TRNSYS, 1990, *A Transient System Simulation Program,*, Solar Energy Laboratory, University of Wisconsin-Madison, Madison, Wisconsin, Sept.